Broadband Proton Decoupling in Human ^{31}P NMR Spectroscopy

Peter R. Luyten,† Gerard Bruntink, Frenk M. Sloff, Jan W. A. H. Vermeulen, Jan I. van der Heijden, Jan A. den Hollander and Arend Heerschap
Philips Medical Systems, PO Box 10.000, NL-5680 DA Best, The Netherlands

The limited chemical shift dispersion of *in vivo* ^{31}P NMR spectra obtained at the relatively low field strengths used for human applications is the cause of poor spectral resolution. This makes it difficult to obtain accurate quantitative information from overlapping resonances, and interesting resonances may be obscured. At 1.5 T unresolved ^{1}H–^{31}P couplings contribute significantly to the linewidth of *in vivo* ^{31}P NMR resonances. Therefore, proton decoupling can improve spectral resolution substantially, resulting in better resolved resonances and more reliable quantitative information. In this work it is shown that well resolved resonances of glycerophosphocholine, glycerophosphoethanolamine and phosphoethanolamine are obtained in ^{1}H decoupled ^{31}P NMR spectra of human muscle, brain, and liver. In spectra of the human heart it has been possible to resolve the myocardial P_i signal from the signals of 2,3-diphosphoglycerate from blood. With surface coils it is difficult to achieve broadband decoupling over the entire sensitive region of the coil by using conventional decoupling sequences. This problem has been overcome by applying a train of frequency modulated inversion pulses to achieve proper decoupling despite B_2 inhomogeneity. Broadband ^{1}H decoupling of ^{31}P NMR spectra was possible without exceeding specific absorption rate guidelines.

INTRODUCTION

Over a number of years, *in vivo* ^{31}P NMR spectroscopy has been used to study the metabolism of intact tissues. With the increased availability of whole body NMR instruments there has been a rapidly growing interest in the application of ^{31}P NMR spectroscopy to non-invasive examination of human tissues and organs. In most applications of human spectroscopy, surface coils are used for spatial selection, which restricts the method to ^{31}P NMR studies of relatively superficial tissues. However, over the past several years techniques have become available to obtain spatially localized ^{31}P NMR spectra of deeper lying human tissue and organs.[1] The phase-encoding method[2] has recently been applied to acquire a large number of spectra from the human brain or organs within an acceptable measurement time.[3]

Intracellular pH and energy metabolism can be monitored by measuring the inorganic phosphate (P_i), phosphocreatine (PCr) and ATP signals. Furthermore, the phosphomono- and di-ester signals in the ^{31}P NMR spectrum monitor anabolic and catabolic intermediates of phospholipid metabolism, which may change in rapid cell growth and degenerative diseases.

In a number of pathological conditions, changes in ^{31}P NMR spectra are quite small, and excellent signal-to-noise ratio and spectral resolution are required to measure them. Because of the low intrinsic sensitivity of ^{31}P NMR the signal-to-noise ratio of *in vivo* spectra tends to be poor, while good spectral resolution is often not achieved by the present localization and spectroscopic imaging techniques. As a result questions have been raised about the utility of ^{31}P NMR for clinical application. The inherently low signal strength of the ^{31}P NMR signal requires relatively large volumes of interest, which makes the method unsuitable for the detection of small focal abnormalities or tissue heterogeneities. Furthermore, the chemical shift dispersion at 1.5–2 T is too small to resolve all the different resonances which makes accurate quantification difficult. Recently whole-body magnets of up to 4 T have become available, providing a new perspective to the application of NMR spectroscopy to humans. However, since most whole-body NMR instruments available at the present time operate at 1.5 T it is also important to optimize the performance of human spectroscopy at that field.

Poor spectral resolution at 1.5 T may in part be overcome by optimizing the magnetic field homogeneity over the volume of interest. For this purpose it is essential to combine ^{31}P NMR localization schemes with single shot ^{1}H NMR volume selection methods in order to shim the water resonance over the volume of interest. At 1.5 T the tissue water resonance may be shimmed to within 0.1–0.3 ppm, resulting in ^{31}P NMR line widths of the order of 3–7 Hz. At these line widths, the 3 bond isotropic coupling between protons and phosphorous may become the dominant factor in the residual resonance linewidth of ^{31}P nuclei coupled to one or more protons, such as in 2,3-diphosphoglycerate (2,3-DPG), nicotinamide adenine dinucleotide (NAD^+), phosphoethanolamine (PE), phosphocholine (PC), glycerophosphoethanolamine (GPE), glycerophosphocholine (GPC) and alpha ATP. In earlier animal studies the 5–10 Hz isotropic J

† Author to whom correspondence should be addressed.
A preliminary account of this work was presented at the 7th Annual Meeting of the Society of Magnetic Resonance in Medicine, San Francisco, 20–26 August 1988, abstracts 708 and 833.

CCC–0952–3480/89/0177–0183 $03.50

couplings between ^{31}P and ^{1}H were considered to be negligible compared to the intrinsic ^{31}P NMR linewidths observed in *in vivo* spectra. Although ^{1}H decoupling has been applied in ^{31}P NMR studies of cell suspensions it has not been regarded as a tool by which there is much to be gained in ^{31}P NMR spectroscopy of humans and animals. Because of the excellent magnetic field homogeneity that can be achieved by local shimming techniques this is no longer true for human spectroscopy at the relatively low field strength of 1.5 T.

In this study it is demonstrated that improvement in spectral resolution can be achieved by combining (localized) ^{31}P NMR spectroscopy with ^{1}H decoupling. To improve the performance of proton decoupling with surface coils a frequency modulated (FM) decoupling sequence was implemented, which provides optimal decoupling irrespective of variations in B_2. ^{1}H decoupled localized ^{31}P NMR spectra were obtained of human muscle, brain, liver, and heart. In these spectra it has been possible to identify resonances which were not resolved before.

EXPERIMENTAL

Hardware. The measurements were performed on a whole body 1.5 T Philips Gyroscan NMR scanner, which was equipped with a second transmit channel for ^{1}H decoupling. Magnet and gradient set were supplied by Oxford Magnet Technology. The standard eddy current compensation was applied.

To obtain proton decoupled ^{31}P NMR spectra of human muscle, liver, and heart, a double surface coil configuration was used. A 14 cm diameter circular surface coil was employed for ^{31}P NMR, and a 16 cm diameter rectangular butterfly coil[4] for ^{1}H decoupling. The ^{31}P and the ^{1}H coils were mounted in a parallel fashion, and were centered with respect to each other. This configuration of the circular ^{31}P coil and the ^{1}H butterfly coil minimizes inductive coupling between the two coils, to provide a better performance of the decoupling experiment. The ^{1}H coil was positioned 4.5 cm further away from the tissue than the ^{31}P coil, in order to prevent excessive RF power absorption in the high flux regions close to the decoupling coil.

For studies of the human head we used a ^{31}P RF coil consisting of two loops of 18 cm in diameter in a Helmholtz configuration, placed at either side of the head. This coil was used in combination with a regular 30 cm diameter ^{1}H head coil for imaging and decoupling; the two coils had an orthogonal configuration to reduce inductive coupling.

Shimming and localization. Excellent magnetic field homogeneity is a pre-requisite for the experiments described here. To achieve this, it is necessary to shim the magnetic field over the region of interest. Shimming was performed by monitoring the ^{1}H resonance of tissue water from the region of interest, by using a single-shot volume selection technique; the volume selection technique used was derived from stimulated echo volume selection.[5–8] The bandwidth of the selective RF pulse used for ^{1}H volume selection was 1250 Hz; for a selected volume size of 3–10 cm this corresponds to a selection gradient ranging from 10 to 3 gauss/m. Gradient rise time used was 1.5 ms. The water resonance was shimmed to less than 0.1 ppm for examinations of the human brain, and to 0.2–0.3 ppm for human liver and heart.

To obtain localized ^{31}P NMR spectra the ISIS sequence[9–12] was employed. By using adiabatic rapid passage inversion[15–20] and excitation pulses[21] the technique has been adapted for surface coils.[10–12] For volumes of up to 6 cm in diameter a gradient strength of 30 gauss/m is used, while the bandwidth of the selection pulse is adjusted to obtain the required volume size. For volume sizes larger than 6 cm a selection bandwidth of 3060 Hz is used, while the gradient strength is adjusted. A 5 ms delay was included between selection gradients and excitation to reduce possible deterioration of spectral resolution by gradient-induced eddy currents.

Proton decoupling. Many different pulse schemes have been proposed in high resolution NMR to obtain effective proton decoupling, mainly for proton decoupled ^{13}C NMR spectroscopy.[13] To a certain extent these sequences have been designed assuming homogeneous B_2 decoupling fields. Since the ^{1}H head coil used for proton decoupling of the human head generates a homogeneous B_2 field, proton decoupling could be achieved by a regular WALTZ-4 sequence, using a basic 90 degree pulse length of 900 μs, corresponding to an expected decoupling bandwidth of $\pm$280 Hz around the water resonance. Using a recycle delay of 3.5 s and gating the decoupler only on during the 260 ms acquisition time the average RF decoupling power applied was 1.4 watt. With the conservative assumption that this power is all absorbed by the tissue this leads to an estimated specific absorption rate (SAR) of 0.5 W/kg, well within the FDA guideline of 3.2 W/kg. For this calculation it has been assumed that power is absorbed evenly by a total of 3 kg tissue within the headcoil.

When used with adequately dimensioned surface coil pairs the WALTZ-16 sequence may still achieve adequate decoupling despite B_2 inhomogeneity.[14] However, for optimal decoupling performance with surface coils the RF pulses have to be adjusted for the particular region of interest. When using localization techniques and decoupling in combination with surface coils this would require pulse adjustments both for B_1 and B_2, in order to obtain optimal spectral localization and decoupling for the region of interest. By using an ISIS technique[9] in which frequency modulated adiabatic rapid passage pulses are employed[10–12] both for the selective inversion[15–20] and for the non-selective detection pulses,[21] this B_1 dependence has been eliminated for the observe channel.

Proton decoupling requires repeated inversion of the proton spins, by applying proton inversion pulses with a repetition time short compared to 1/J. The small ^{31}P–^{1}H indirect coupling constants allow for a relatively slow rate at which the proton spins have to be inverted to achieve decoupling. Thus although the

hyperbolic secant frequency modulated inversion pulses are rather long, these pulses can still generate proton inversions fast enough to decouple these small couplings. Moreover, the protons involved are confined to a relatively small chemical shift range, thus only a limited decoupling bandwidth is needed. This suggests that a B_2 insensitive decoupling sequence can be implemented by applying a train of hyperbolic secant inversion pulses. The individual pulses used in this work had a length of 8 ms, corresponding to a spectral width of ±580 Hz centered around the water resonance in the ^{1}H NMR spectrum.

Using this B_2 independent decoupling sequence, excellent proton decoupling of the ^{31}P NMR spectra could be obtained over the entire sensitive volume of the ^{31}P surface coil, using a peak power of 140 watt. The decoupling sequence was only applied during acquisition of the ^{31}P NMR spectrum, and was gated off during the recycle delay period. With an acquisition time of 256 ms and a repetition time of 3 s this gives rise to an average applied decoupling power of 3.7 watt. Power absorption in the surface coil decoupling experiment is distributed unevenly over the exposed tissue, because of B_2 inhomogeneity. In order to estimate the highest power absorption in any 1 g of tissue the following calibration was performed. The peak power was determined that was required to generate a 90 degree pulse of 400 μs with a head coil which was loaded with the leg of a volunteer. Power absorbed by the tissue was determined by measuring the Q-factors of the coil, loaded and unloaded. In this way it was determined that peak power absorption was 20 W/kg for a 90 degree pulse of 400 μs. Next we determined how much power is required to generate a 400 μs 90 degree pulse at the tissue surface when using the surface coil assembly. Assuming that the SAR is always the same for a given RF field strength we can now calculate the SAR at the surface by using the following formula:

$$P_{sup} = (P_{av}/P_{90}) \times 20,$$

in which P_{av} is the average power applied in the decoupling sequence, and P_{90} is the peak power required for a 400 μs 90 degree pulse at the surface. From this we obtain a SAR at the surface $P_{sup} = (3.7/40) \times 20 = 1.85$ W/kg. This shows that the average power level needed for the FM decoupling sequence is moderate compared to the power required for WALTZ decoupling. The FM decoupling sequence inverts protons only once every 8 ms, whereas in the WALTZ sequence the rate of inversion is at least 4 times higher; this lower rate of proton inversion makes up for the higher power needed for the FM inversion pulses. For the WALTZ sequence a high rate of inversion is required in order to obtain the required decoupling bandwidth. The average power applied for the ISIS sequence is about 0.25 W, which is low compared to the average applied decoupling power.

Data processing. The FID's were windowed using Lorentz–Gauss multiplication. Gaussian multiplication was applied with a linebroadening of 3–7 Hz, followed by multiplication with a positive exponential corresponding to a line narrowing of 3–6 Hz. This procedure leads to an effective linebroadening of 1 Hz or less. Convolution difference was applied to remove broad components (i.e., 200 Hz linebroadening was applied, and 0.9 times the result of that was subtracted from the original data). Data were zerofilled to 2 K, and a FFT was applied followed by a linear phase correction.

Quantitative analysis of the data was performed by fitting with a model function in the time domain.[22] The model function used consisted of a sum of exponentially damped sinusoids. Fast least squares model fitting is possible by exploiting the mathematical properties of the exponential model function.[23] From the fitting procedure the peak areas, chemical shifts, and linewidths are obtained. The lower bounds of the standard deviations of the spectral parameters can be calculated for a given noise level by using the Cramer–Rao theory.[24,25] These Cramer–Rao lower bounds are exclusively determined by the magnitude of the noise, and the values of the spectral parameters; they provide a realistic estimate of the variation in spectral parameters from *in vivo* ^{31}P NMR spectra.[26]

RESULTS

Skeletal muscle

Figure 1 shows two ^{31}P NMR spectra of human calf muscle taken with a 14 cm diameter surface coil. The spectrum is the average of 64 measurements with a recycle delay of 3 s, using an adiabatic half passage excitation pulse without volume selection. The

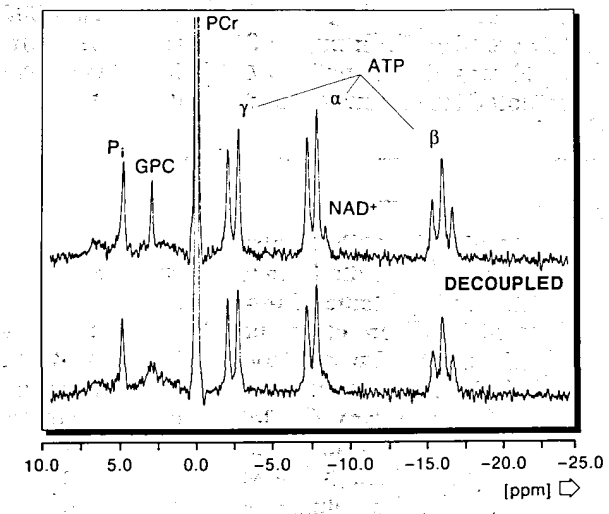

Figure 1. 1.5 T ^{31}P NMR spectra of the human calf. The spectra were obtained in 64 scans and a repetition time of 3 s with a 14 cm diameter surface coil, using an adiabatic rapid half passage excitation pulse without spatial localization. The lower spectrum was obtained without proton decoupling, the upper trace with it. Decoupling was done using a train of FM inversion pulses, applied through a separate ^{1}H surface coil. The decoupled spectrum shows a well resolved resonance from GPC, which is barely discernible in the non-decoupled spectrum. Also note the increase in signal-to-noise. The PCr signal is off-scale in both spectra.

Table 1. Peak areas of the individual spectral components, normalized to β-ATP

	Calf muscle	Liver	Brain	Heart
PME	0.39 ± 0.05	1.07 ± 0.17	0.47 ± 0.08	—
P_i	0.43 ± 0.03	0.78 ± 0.12	0.56 ± 0.08	0.19 ± 0.05
GPE	0.04 ± 0.02	0.56 ± 0.10	0.11 ± 0.05	—
GPC	0.32 ± 0.03	0.29 ± 0.08	0.16 ± 0.04	—
PCr	3.54 ± 0.14	—	0.99 ± 0.01	1.37 ± 0.09
γ ATP	1.02 ± 0.04	1.17 ± 0.18	1.21 ± 0.24	0.99 ± 0.08
α ATP	1.17 ± 0.05	1.37 ± 0.28	1.21 ± 0.24	1.38 ± 0.11†
DPDE	0.10 ± 0.02	0.85 ± 0.28	0.10 ± 0.03	—
Chemical shift				
P_i (ppm)	4.866 ± 0.007	5.15 ± 0.02	4.86 ± 0.01	4.89 ± 0.02

The peak areas were determined by least-squares fitting to a time domain model function, which consisted of a sum of exponentially damped sinusoids.[23] The relative intensities are not corrected for partial saturation effects. Also given is the P_i chemical shift as determined by the fitting procedure. The standard deviations provided are the lower bounds calculated by the Cramer–Rao theory.
† Includes DPDE.

non-decoupled spectrum shows the familiar signals of P_i, a very intense PCr (off scale), and three ATP signals. The ^{31}P–^{31}P couplings (16–17 Hz) are clearly resolved in the ATP phosphate signals, which demonstrates the excellent field homogeneity in this measurement. In the proton decoupled spectrum a remarkable improvement in signal-to-noise and spectral resolution is obtained for alpha ATP, NAD^+ and the phosphodiester region. In the phosphodiester region a distinct resonance has appeared, which was assigned to GPC on the basis of its chemical shift.

Using a non-linear fitting time domain procedure,[23] peak areas and peak positions were determined for the proton decoupled ^{31}P NMR spectrum. The peak areas are given in Table 1; the peak position of the P_i and GPC peaks relative to PCr were 4.866 ± 0.007 and 2.97 ± 0.01 ppm. From the P_i–PCr chemical shift, tissue pH was determined to be 7.057 ± 0.006. All errors quoted are Cramer-Rao standard deviations.

Liver

An example of a spatially localized proton decoupled ^{31}P NMR spectrum of the liver is presented in Fig. 2. This spectrum was obtained from a selected volume of 300 cm^3 in the liver of a healthy volunteer by accumulating 280 FID's with a repetition time of 3 s, using a 14 cm diameter surface coil. For localization the ISIS technique was employed, using adiabatic inversion and detection pulses. Shimming was performed by monitoring the ^1H NMR resonance of tissue water from the volume of interest by a single shot localization scheme using stimulated echoes.[5–8] The ^{31}P NMR spectrum shows two well-resolved resonances in the phosphodiester region which have been assigned to GPE and GPC. Also, the phosphocholine signal and diphosphodiesters are better resolved than in the non-decoupled human liver spectrum. The small residual PCr signal is due to skeletal muscle in the fringe regions adjacent to the region of interest. An additional advantage of the

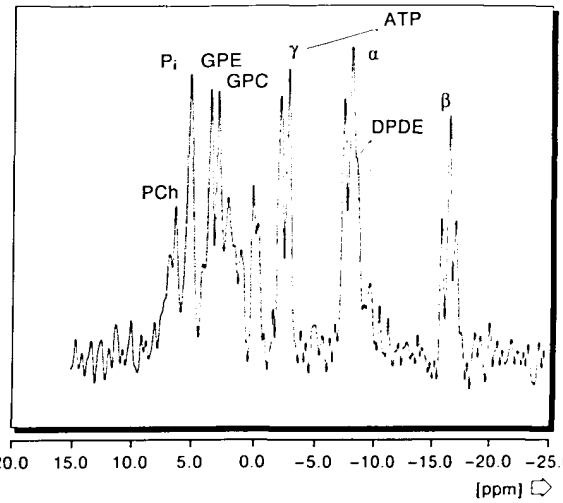

Figure 2. Proton decoupled localized ^{31}P NMR spectrum of the human liver, obtained at 1.5 T, using a 14 cm diameter surface coil. The localization scheme used was ISIS with FM inversion and excitation pulses. The spectrum was obtained in 280 scans with 3 s repetition time. Proton decoupling has improved resolution in the phosphodiester, phosphomonoester, and diphosphodiester region. Well resolved resonances are observed of GPE, GPC, and PCh.

increased resolution between the spectral lines is the higher accuracy by which the P_i peak position, and thus intra cellular pH, is determined. Moreover, the clearly resolved GPC resonance can be used as an internal reference for chemical shift determination, whereas previously no suitable reference for this purpose was at hand in localized liver spectra. Using GPC as a reference at 2.97 ppm from PCr, the P_i is found to be at 5.15 ± 0.02 ppm, from which a tissue pH of 7.32 ± 0.02 is derived. Errors quoted are Cramer-Rao standard deviations. Peak areas as determined from the spectrum are given in Table 1.

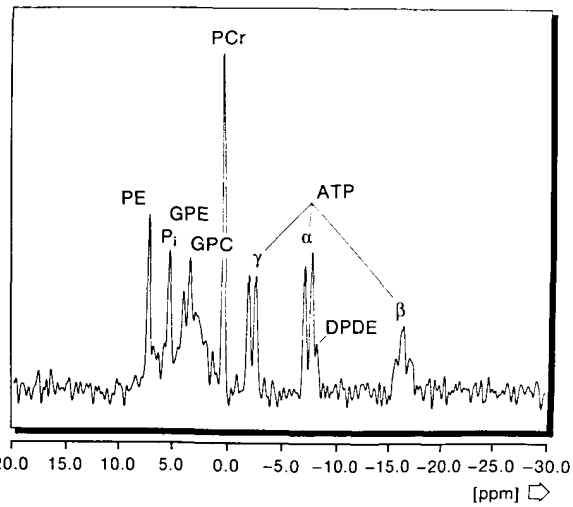

Figure 3. Proton decoupled ^{31}P NMR spectrum of the brain of a 6 year old girl, who has a history of chemotherapy for leukaemia. The spectrum was obtained using a small ^{31}P NMR headcoil, and a regular ^1H imaging headcoil for decoupling. WALTZ-4 decoupling was applied; the spectrum was obtained in 256 scans, with 3.5 s repetition time. Proton decoupling has helped to resolve resonances from GPC, GPE, PE, and NAD^+.

Brain

A localized proton decoupled ^{31}P NMR brain spectrum is shown in Fig. 3. A ^{31}P Helmholtz coil of 18 cm diameter was used, with a regular ^{1}H head coil. This spectrum was obtained from the left cerebral hemisphere of a 6-year-old girl with a history of leukaemia and chemotherapy treatment. The volume size was 200 cm^3, and the spectrum was obtained in 256 measurements, using a recycle delay of 3.5 s. Pronounced PE and well resolved GPC and GPE resonances are observed, which demonstrate the improved spectral resolution. The peak positions relative to PCr in this spectrum are 2.97 ± 0.01 ppm for GPC, 3.51 ± 0.02 for GPE, 4.86 ± 0.01 for P_i and 6.77 ± 0.01 for PE. The errors are the Cramer–Rao lower bounds. Using the titration data given by Petroff *et al.*,[27] a pH value of 7.05 ± 0.01 is calculated from the chemical shift position of the P_i peak. Peak areas from the spectrum are given in Table 1.

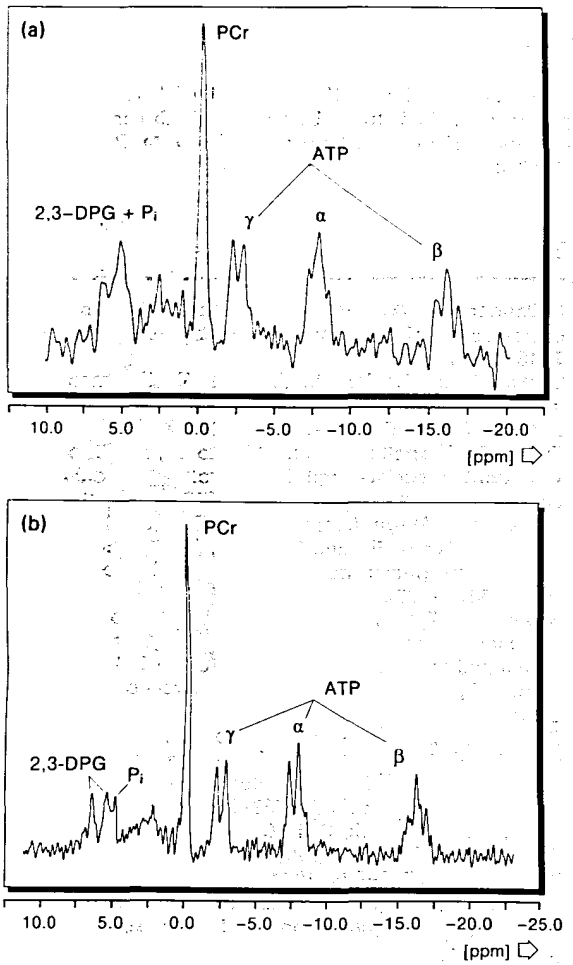

Figure 4. (a) 1.5 T localized ^{31}P NMR spectrum of the human heart. The spectrum was obtained with a 14 cm diameter surface coil, using ISIS localization with frequency modulated inversion and excitation pulses. In this non-decoupled spectrum the region of 4–7 ppm shows an unresolved resonance from 2,3-DPG, and P_i. (b) Proton decoupled ^{31}P NMR spectrum of the human heart. In this spectrum the spectral region of 4–7 ppm has been resolved into two resonances of 2,3-DPG (P2 at 6.4 ppm, and P3 at 5.4 ppm), and a resonance of P_i (4.89 ppm). The P_i chemical shift corresponds to a pH of 7.14, which is characteristic for myocardium.

Heart

Heart spectra were obtained using a 14 cm diameter surface coil. Figure 4a shows a localized ^{31}P NMR spectrum of the human heart obtained at 1.5 tesla, with no proton decoupling. The spectral region of 4–6 ppm shows a broad resonance, which can be attributed to contributions from the 2 and the 3 phosphate of 2,3-DPG from blood, and from P_i. In this spectrum the P_i signal is obscured, and as a result it is not possible to quantify the P_i signal, nor is it possible to derive an accurate pH value for the myocardium. Thus in this particular case, very important information is lost in these spectra because of spectral overlap. This problem has been addressed before by attempting to use spin editing techniques to suppress the 2,3-DPG signal.[28] The 9 Hz proton coupling in the P-2 doublet and 5.6 Hz coupling in the P-3 triplet of 2,3-DPG require transverse evolution times that are long compared to the relatively short T_2 values of the several ^{31}P NMR signals. However, proton decoupling can be used to enhance the resolution of the 2,3-DPG signals, uncovering the P_i peak usually obscured by the resonances of 2,3-DPG. Figure 4b shows a proton decoupled localized ^{31}P NMR human heart spectrum. The spectrum is from a $9 \times 9 \times 2.5$ cm volume of interest, which was positioned over the left ventricular wall. The spectrum was acquired in 768 scans, using a minimal repetition time of 3 s combined with triggering 250 ms after the R wave of the ECG signal. Peak areas are given in Table 1. A small P_i resonance at 4.89 ± 0.02 ppm can be observed next to the resonance of P-3 of 2,3-DPG. The Cramer-Rao standard deviation for the area of this signal is 26% (Table 1). Tissue pH derived from this P_i chemical shift is 7.14, which agrees with pH values found for perfused hearts;[29] pH values for serum are known to be higher than this. Furthermore, the PCr/ATP, and P_i/PCr ratios are as expected for myocardium, which confirms that this P_i signal can be attributed to the myocardium.

DISCUSSION

We have demonstrated that the information content of human ^{31}P NMR spectra obtained at relatively low field strengths improves significantly by using proton decoupling. In particular, much more information is obtained from the phosphomono- and di-ester regions. It is now possible to observe well-resolved resonances of PC, PE, GPE, GPC, and other relevant resonances in these spectral regions. These signals may play a very important role in assessing biochemical processes which take place in ageing, tumour growth and many diseases which involve changes in the turnover of membrane components. The clearly resolved GPC resonance which was identified in spectra of human muscle, brain, and liver provides an alternative to PCr as an accurate internal reference for calibrating human ^{31}P NMR chemical shifts. This is important, not only for liver or tumour spectra where PCr is absent, but also in spectra of muscle where PCr may become a less reliable

reference due to its titration behaviour under acidotic conditions as may occur during stress tests. GPC is known not to change its chemical shift over the physiological pH range.[30] In addition to providing a reliable internal chemical shift reference, proton decoupling also enhances the accuracy of noninvasive pH determinations by ^{31}P NMR, since the overlap between the P_i signal and the unresolved PME and PDE peaks in non-decoupled spectra may lead to less accurate chemical shift determinations. In the proton decoupled ^{31}P NMR spectra presented here, the peak position of the P_i resonance was determined with an accuracy of 0.005–0.02 ppm, which allows tissue pH to be determined to within 0.01. These standard deviations are the lower bounds calculated by the Cramer-Rao theory.[24,25] In ^{31}P NMR spectra of the heart, the P_i resonance may be resolved from the 2,3-DPG signals, which makes it possible to measure pH of the human myocardium.

In addition to more accurate chemical shift determination of better resolved resonances, it is also possible to determine peak areas with a higher accuracy for the measurement of metabolite concentrations. As an example Table 1 gives the relative signal areas as obtained by time domain model function analysis[23] of the proton decoupled ^{31}P NMR spectra shown in this study. All signal integrals listed are normalized to beta-ATP, not corrected for partial saturation effects. The Cramer-Rao lower bounds on the standard deviations are also given in the Table.

The application of a train of adiabatic rapid passage inversion pulses results in a decoupling sequence that can be used for uniform decoupling over the entire sensitive region of the surface coil. Above a certain threshold the decouple performance is independent of the power level. The power level required for *in vivo* ^{1}H decoupling of ^{31}P NMR signals at 1.5 T are quite moderate and can be kept within the SAR guidelines recommended for human examination.

The improvement in human ^{31}P NMR spectra obtained by proton decoupling raises questions about optimal field strengths for human spectroscopy. Since the SAR increases with frequency, broadband ^{1}H decoupling may not be feasible at higher field within the present guidelines. Furthermore, decoupling at higher field strengths will be less effective in improving ^{31}P NMR spectral resolution, as the *in vivo* line broadening increases at higher field because of tissue susceptibility effects.

Acknowledgement

The authors thank Dr A. Kingma and Dr W. A. Kamps of the Department of Pediatrics, University of Groningen for their collaboration. The technical assistance of L. J. M. P. Oosterwaal is appreciated.

REFERENCES

1. Aue, W. P., Localization methods for *in vivo* nuclear magnetic resonance spectroscopy. *Rev. Magn. Reson. Med.* **1,** 21–72 (1986).
2. Brown, T. R., Kincaid, B. M., and Ugurbil, K., NMR chemical shift imaging in three dimensions. *Proc. Natl. Acad. Sci. USA* **79,** 3523–3526 (1982).
3. Bailes, D. R., Bryant, D. J., Bydder, G. M., Case, H. A., Collins, A. G., Cox, I. J., Evans, P. R., Harman, R. R., Hall, A. S., Khenia, S., McArthur, P., Oliver, A., Rose, M. R., Ross, B. D., and Young, I. R., Localized phosphorus-31 NMR spectroscopy of normal and pathological human organs *in vivo* using phase-encoding techniques. *J. Magn. Reson.* **74,** 168–170 (1987).
4. Sobol, W. T., Dedicated coils in magnetic resonance imaging. *Rev. Magn. Reson. Med.* **1,** 181–224 (1986).
5. McKinnon, G., Localized double quantum filter and correlation spectroscopy experiments. *Magn. Reson. Med.* **6,** 332–343 (1988).
6. Frahm, J., Merboldt, K. D., and Hänicke, W., Localized proton spectroscopy using stimulated echoes. *J. Magn. Reson.* **72,** 502–508 (1987).
7. Granot, J., Selected volume excitation using stimulated echoes (VEST) applications to spatially localized spectroscopy and imaging. *J. Magn. Reson.* **70,** 488–492 (1986).
8. Kimmich, R., and Hoepfel, D., Volume-selective multipulse spin-echo spectroscopy. *J. Magn. Reson.* **72,** 379–384 (1987).
9. Ordidge, R. J., Connelly, A., and Lohman, J. A. B., Image-selected *in vivo* spectroscopy (ISIS). A new technique for spatially selective NMR spectroscopy. *J. Magn. Reson.* **66,** 283–294 (1986).
10. Luyten, P. R., Groen, J. P., Vermeulen, J. W. A. H., and den Hollander, J. A., Experimental approaches to image localized human ^{31}P NMR spectroscopy. *Magn. Reson. Med.* in press.
11. Segebarth, C., Balériaux, D., Arnold, D. L., Luyten, P. R., and den Hollander, J. A., MR image-guided P-31 MR spectroscopy in the evaluation of brain tumor treatment. *Radiology,* **165,** 215–219 (1987).
12. Segebarth, C., Grivegnée, A., Luyten, P. R., and den Hollander, J. A., ^{1}H image-guided localized ^{31}P MR spectroscopy of the human liver. *Magn. Res. Med. Biol.* **1,** 7–16 (1988).
13. Shaka, A. J., Keeler, J., Frenkiel, T., Freeman, R., An improved sequence for broadband decoupling: WALTZ-16. *J. Magn. Reson.* **52,** 335–338 (1983).
14. Tiffon, B., Mispelter, J., and Lhoste, J., A carbon 13C *in vivo* double surface coil NMR probe with efficient low power proton decoupling at 400 MHz using the waltz16 sequence. *J. Magn. Reson.* **68,** 544–550 (1986).
15. Baum, J., Tycko, R., and Pines, A., Broadband population inversion by phase modulated pulses. *J. Chem. Phys.* **79,** 4643–4644 (1983).
16. Baum, J., Tycko, R., and Pines, A., Broadband and adiabatic inversion of a two-level system by phase modulated pulses. *Phys. Rev. A* **32,** 3435–3447 (1985).
17. Tycko, R., Broadband population inversion. *Phys. Rev. Letters* **51,** 775–777 (1983).
18. Silver, M. S., Joseph, R. I., and Hoult, D. I., Selective spin inversion in nuclear magnetic resonance and coherent optics through an exact solution of the Bloch-Ricati equation. *Phys. Rev. A* **31,** 2753–2755 (1985).
19. Silver, M. S., Joseph, R. I., Chen, C.-N., Sank, V. J., and Hoult, D. I., Selective population inversion in NMR. *Nature (London).* **310,** 681–683 (1984).
20. Silver, M. S., Joseph, R. I., and Hoult, D. I., Highly selective pi/2 and pi pulse generation. *J. Magn. Reson.* **59,** 347–351 (1984).
21. Bendall, M. R., and Pegg, D. T., Uniform sample excitation with surface coils for *in vivo* spectroscopy by adiabatic rapid half passage. *J. Magn. Reson.* **67,** 376–381 (1986).
22. van der Veen, J. W. C., de Beer, R., Luyten, P. R., and van Ormondt, D., Accurate quantification of *in vivo* ^{31}P NMR signals using the variable projection method and prior knowledge. *Magn. Res. Med.* **6,** 92–98 (1988).
23. de Beer, R., van Ormondt, D., and Pijnappel, W. W. F., Improved harmonic retrieval from noisy signals by invoking prior knowledge. In: *Signal Processing IV: Theories and Applications,* ed. by J. L. Lacoume, A.

Chehikian, N. Martin, and J. Malbos pp. 1283–1286 Elsevier, Amsterdam. (1988).
24. van den Bos, A., In: *Handbook of Measurement Science* Vol. 1. ed. by P. Sydenham, pp. 331–377. Wiley, Chichester (1982).
25. Barkhuysen, H., de Beer, R., and van Ormondt, D., Error theory for time-domain signal analysis with linear prediction and singular value decomposition. *J. Magn. Reson.* **67,** 371–375 (1986).
26. de Beer, R., den Hollander, J. A., Mariën, A. J. H., van Ormondt, D., and Segebarth C. M., Evaluation of the reproducibility of spectral parameters obtained by quantitative analysis of *in vivo* NMR spectra, *7th Annual Meeting of the Society of Magnetic Resonance in Medicine,* 303, (1988).
27. Petroff, O. A. C., Prichard, J. W., Behar, K. L., Alger, J. R., den Hollander, J. A., and Shulman, R. G., Cerebral intracellular pH by ^{31}P nuclear magnetic resonance spectroscopy. *Neurology,* **35,** 781–788 (1985).
28. Brindle, K. M., Rajagopalan, B., Bolas, N. M., and Radda, G. K., Editing of ^{31}P spectra of heart *in vivo. J. Magn. Reson.* **74,** 356–365 (1987).
29. Flaherty, J. T., Weisfeldt, M. L., Bulkley, B. H., Gardner, T. J., Gott, V. L., and Jacobus, W. E., Mechanisms of ischemic myocardial cell damage assessed by phosphorus-31 nuclear magnetic resonance, *Circulation* **65,** 561–571 (1982).
30. Navon, G., Ogawa, S., Shulman, R. G., and Yamane, T., ^{31}P nuclear magnetic resonance studies of Ehrlich ascites tumor cells, *Proc. Natl. Acad. Sci. USA* **74,** 87–91 (1977).

Received 9 September 1988; accepted (revised) 4 October 1988.